A tale of two realities: reconciling physical and numerical modeling via 'bootstrap' processing

David C. Henley

ABSTRACT

Seismic physical modeling is the process of conducting seismic surveys on laboratory scale models of earth structures, using ultrasonic transducers, to simulate the expected seismic response to similar structures in the earth. From modeling results, we improve our understanding of the generation and propagation of various elastic and acoustic wave modes in the real earth. Because of the similarity to seismic field surveying, physical model results can be considered a form of 'ground truth' for geology accurately represented by the model.

Numerical modeling, on the other hand, creates a simulated seismic response to a digital representation of a physical earth structure. It is useful not only for evaluating how well a digital model represents the earth, but also for verifying the modeling process itself. Numerical modeling plays a significant role in Full Waveform Inversion, since a modeling algorithm is used to compute a seismic response to the most current earth model to compare with the most current processed input data, in order to update the model.

Using a scale model constructed and surveyed in the CREWES physical modeling lab, we have the unique opportunity to compare images obtained from the physical model survey data with images produced by the data from numerical modeling of a digital representation of the laboratory scale model. We initially have only a schematic of the laboratory physical model, however, so we first use the schematic, along with an image from the physical survey itself, to create the digital model for input to the numerical modeling algorithm. The physical model data are then re-imaged using this estimated digital model velocity field, and the model itself updated--a 'bootstrap' approach. We then use a finite difference acoustic numerical modeling algorithm to create a CMP survey of the digital model, emulating the acquisition geometry of the actual survey. The numerical data are processed identically to the physical model data. We compare the physical and numerical model images.

INTRODUCTION

Previously, Wong et al (2019) created a physical model to be surveyed in the CREWES physical modeling facility. The model itself simulated a geometrical situation sometimes encountered in exploration, where deep structures of exploration interest are masked by shallow structures of relatively high velocity. As shown in the schematic in Figure 1, the deep structure of the model consists of two high velocity planar layers with smaller dome-shaped structures superimposed. At a much shallower depth is another high velocity structure consisting of a slightly tilted sill and contiguous dike. Because of its high velocity, and the low velocity of the medium separating this structure from the deeper objectives (water), the model presents the classical 'velocity inversion', which is always difficult to process and invert for the underlying velocity structure (the model). The model is immersed

in a rectangular water tank, whose sides and bottom are expected to contribute coherent reflections to the seismic response obtained for this model.

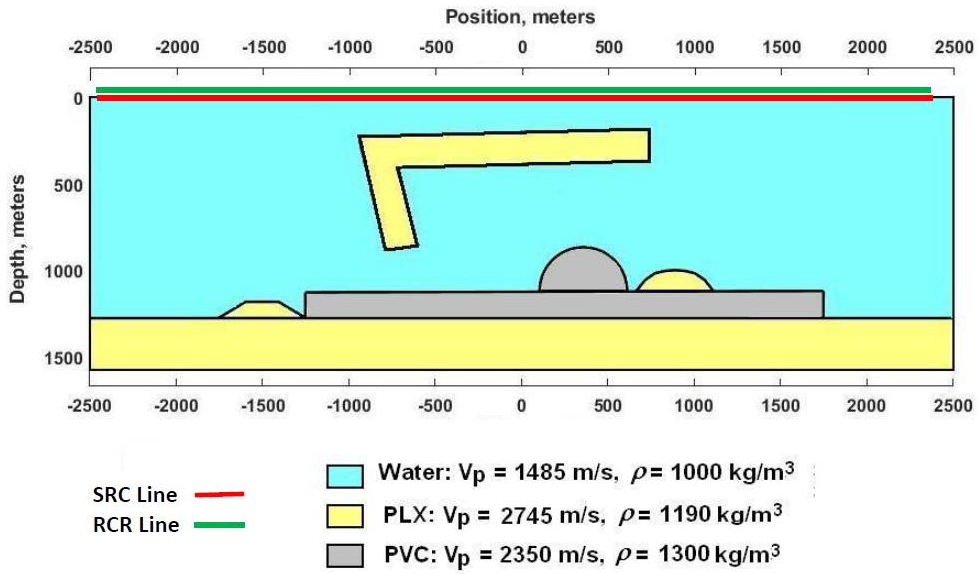

FIG.1. Schematic of physical model showing scaled dimensions as well as material properties.

The dike and sill model was subjected to several types of simulated seismic surveys: a conventional surface based multi-offset CMP survey; a high-resolution 'zero-offset' survey (referred to as a 'sonar' survey); and several surveys in which the sources were in subsurface positions, simulating borehole-based VSP surveys or recording-while-drilling (RWD) surveys. In an earlier report (Henley and Wong 2019), we compared the information obtainable from the sonar survey and that obtainable from the multi-offset CMP survey with minimal processing and analysis. In that report, we concluded that for a quick reconnaissance, the sonar survey reveals a surprising amount of information about the underlying model and its features, and could well provide adequate information for planning further data acquisition and processing, including placement of subsurface sources. In the current work, we begin the process of analyzing and processing the multi-offset CMP data, with the goal to resolve the underlying velocity structure of the physical scale model in the modeling tank.

The first step in obtaining the velocity model for our physical model data is a detailed NMO analysis to yield the best possible RMS velocity model. Using this model, we create the best migrated CMP travel time image of the multi-offset survey and superimpose our 'external knowledge' of the actual model by picking the seismic events representing all known interfaces in the physical model (as shown in the schematic in Figure 1), including 'phantom' interfaces for which there may be no actual seismic response except event terminations. With these horizons picked in travel time space, we can further bring our 'external knowledge' into play by creating an interval velocity vs. time model (VIT), which honours the picked horizons and the known constant velocities in the regions bounded by the horizons. Thus, we use our best RMS velocity model to produce an accurate time image of the data, on which the actual known model horizons can be picked and used with our

knowledge of the material properties of the scale model to create a detailed interval velocity vs. time model. A simple conversion step creates an interval velocity vs. depth model (VID), whose horizons (originally picked on a time section) are then edited to restore the known model boundaries, which have been distorted by the conversion (We use this distorted VID model later in our analysis to test the sensitivity of our numerical modeling to errors in the model).

The interval velocity vs. time model can be converted to RMS velocity vs. time and used for both CMP stacking the physical model and post-stack time migrating it. Additionally, the data can be pre-stack time migrated and compared with the post-stack migration using the same velocities.

The interval velocity vs. depth model is used to apply pre-stack depth migration to the model data. The velocity model can be superimposed on the image to check the fit of the imaged model interfaces with those of the model. We consider the pre-stack depth migration to be the most sensitive test of the underlying velocity model. In most full waveform inversion schemes, there is an algorithm which uses the differences in depth images created from the physical data and the modeling process to apply modifications to the velocity model to decrease the differences. In our study, however, we make no attempt to feed back image differences to modify the model, but simply present the images presented by real data and modeled data when the underlying velocity model is common to both data sets.

To reiterate, in our 'bootstrap' process, we apply conventional processing to the 2D multi-fold ultrasonic survey of the physical model, refining and iterating the velocity analysis until we have a stable time image of the model structure. We then place known model interfaces on the image by picking them on the best time migrated seismic image. The a priori model velocities can be filled between the interface boundaries to form a detailed model of interval velocity in time. This model can then be used to obtain a better pre-stack time migrated image, on which the known model interfaces are re-picked and filled with the model velocities. The interval velocity vs. time model is then directly converted to interval velocity vs. depth, the known model interfaces adjusted to their correct configuration, and this model used to pre-stack migrate the physical data in depth.

The final model, which should be an accurate digital representation of the actual physical model, is supplied to a finite difference modeling algorithm to simulate a 2D multi-fold survey with the same geometry as the actual physical model survey. The two datasets can then be directly compared, since they're based on the same underlying velocity model.

Summary of 'bootstrap' digital model creation

1. Iterative NMO analysis to obtain best possible RMS velocity field from physical model data. Combination of hand picking and autopicking may be necessary.

2. Stack data by CMP, followed by post-stack Kirchhoff migration using best RMS velocity field.

3. Pick known physical model interfaces (a priori information from schematic) on migrated time section.

4. Post the picked interfaces on a blank interval velocity vs. time field (VIT) and infill the known physical model velocities (a priori information). This is the trial interval velocity vs. time field.

5. Convert interval velocity vs. time field to RMS velocity vs. time field. Use this velocity field to re-stack and re-migrate physical model data. Overlay picked horizons on migrated section to check accuracy; and adjust horizons if necessary. Repeat step 4, if necessary.

6. Convert interval velocity vs. time to interval velocity vs. depth field (VID). Adjust horizon boundaries distorted by this operation to their correct configuration and re-fill the velocity volume with the correct velocities. This is the interval velocity vs. depth model. We use this model for all further pre-stack depth migration operations on physical model data, we convert it back to RMS velocities for processing data in time, and we use it as the input for numerical modeling.

PROCEDURE DETAILS

Forward processing of the physical model

Before imaging any seismic data, usually, a certain amount of pre-processing is necessary to attenuate coherent noise, whiten the spectrum, and remove the effects of geometry from the data. Physical model data are no exception to this. Figure 2 shows a raw shot gather from the physical model data set. In addition to the strong direct arrival event, other coherent events are present, corresponding to reflections from the sides and bottom of the modeling tank, some of them out of the 2D acquisition plane. As well, reverberations due to the water surface are present. In Henley and Wong (2019), simple processing steps are described to deal with these issues. The strong direct arrival is attenuated using radial trace (RT) filtering (Henley 2003), the spectrum is whitened, and amplitudes adjusted by Gabor deconvolution (Margrave et al 2011), and reverberations and short period multiples are attenuated via gapped predictive deconvolution. After these steps, the shot gather shown in Figure 2 is shown in Figure 3.

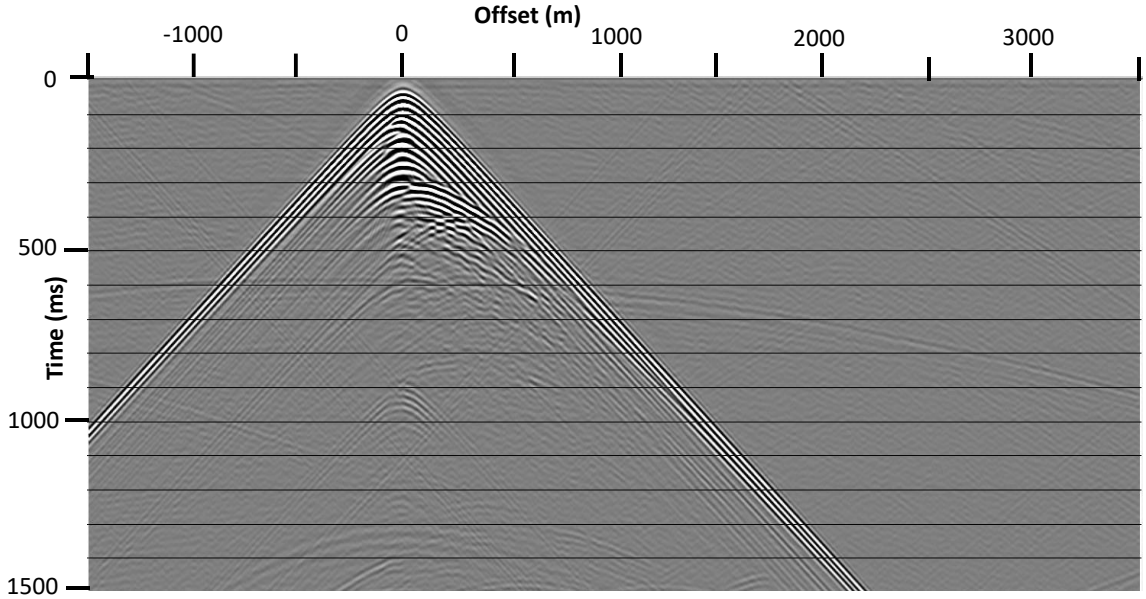

FIG. 2. Raw physical model shot gather from surface location 301. Direct wave dominates the display.

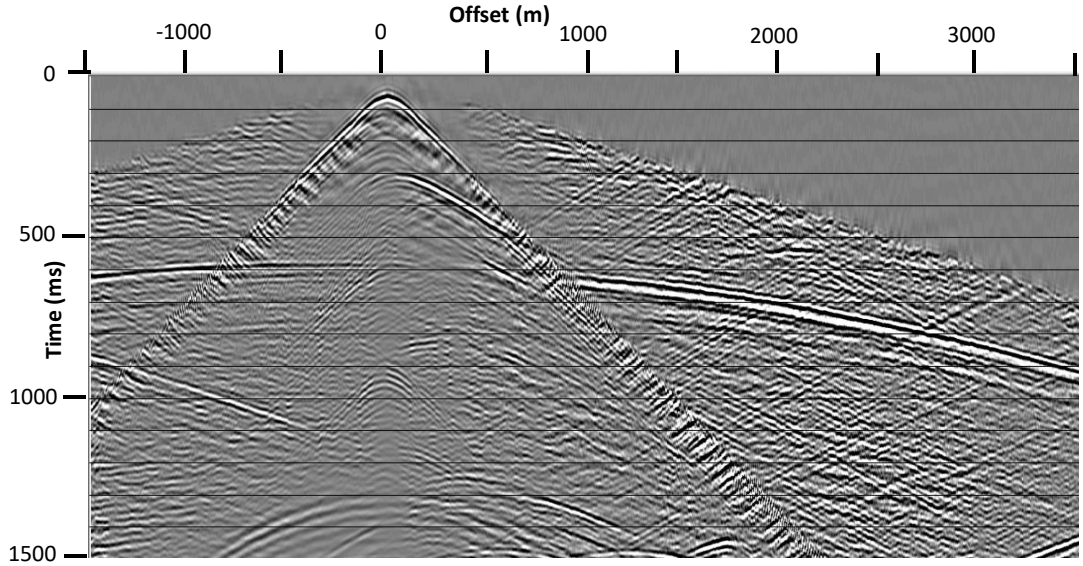

FIG. 3. Physical model shot gather from surface location 301 after RT filter to attenuate water arrival and Gabor deconvolution to whiten spectrum. Out of plane tank-side reflections have not yet been attenuated.

Finally, the data are sorted to the common offset domain, and the broadside reflections from the sides of the tank are removed by subtracting a median-mixed version of the common-offset gather from the raw gather.

In their initial encounter with the multi-fold CMP data set, Henley and Wong (2019) made no attempt to analyze NMO velocities, but simply stacked the data using NMO for water velocity, since water composed the bulk of the model. In this work, we made a significant attempt to analyze moveout on the CMP gathers, using standard NMO picking modules available in SeisSpace. We made multiple attempts to pick the data, using both manual picking and autopicking. Because of the seriously difficult velocity structure of the model, with a major velocity inversion, few legitimate reflections, and lots of diffractions, we found that it took many trials to pick an RMS velocity field which represented primarily legitimate reflections. Whether we used manual picking or autopicking, we found it advantageous to use the results of earlier runs to guide subsequent iterative runs. After 6 iterations each of manual and automatic picking, we chose the autopicked RMS field as the one providing the best NMO correction for known reflections in the physical model data. A plot of this RMS velocity field is shown in Figure 4. Figures 5 and 6 show, respectively, a supergather panel (multiple CMPs) used for the sixth pass of hand picking, and a typical set of semblance panels for the sixth pass of autopicking. The message to be taken from these figures is the difficulty of picking legitimate reflections, as well as the overall sparsity of NMO-conformable events of any kind in these data.

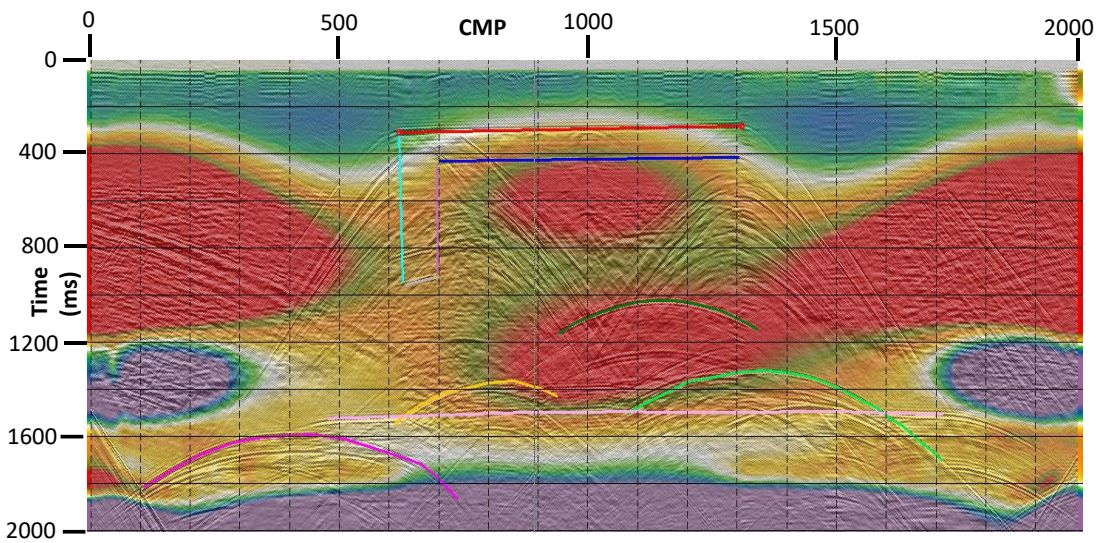

FIG. 4. Best estimate of RMS stacking velocities after six iterations of both hand-picking and autopicking of supergather semblances. Background section is high-resolution zero-offset “sonar” survey. Picked horizons are schematic only. Red = 4000m/s; blue = 1000m/s.

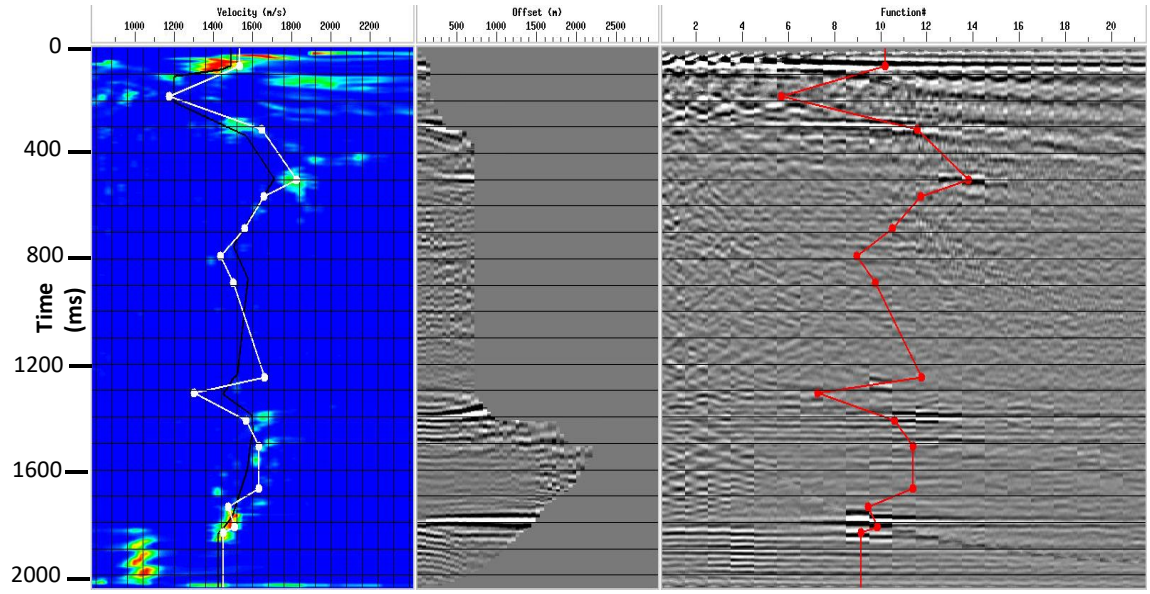

FIG.5. Typical interactive velocity picking panel for supergathers (groups of CMPs) from physical model. Note the sparsity of semblance maxima for these data, due to the relative lack of actual reflecting horizons in the model. This panel is from the sixth iteration of hand-picking, where previous iterations were used to guide the velocity corridor.

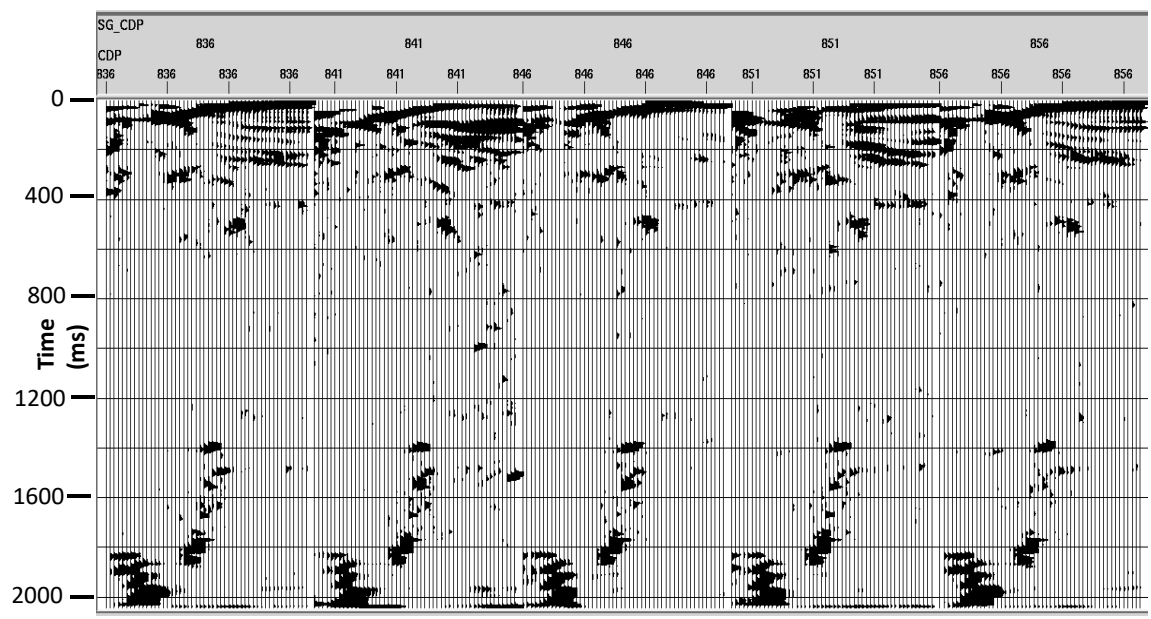

FIG.6. A group of typical supergather (multiple CMP) semblance panels pre-computed for automatic picking. These panels are from the sixth iteration of autopicking, where the previous iterations are used to guide this run. The RMS velocity field in Figure 4 was created from this run.

The velocity field in Figure 4 can be converted to interval velocity vs. time, as shown in Figure 7, but the velocities are unrealistic near the edges, and are difficult to reconcile with known reflection horizons in the model. An attempt to convert to interval velocity vs. depth results in an unusable velocity field with many negative or imaginary values. Hence, we did not use either VIT or VID derived from this VRMS field, but used the VRMS

velocity field only for NMO correction and CMP stacking followed by post-stack Kirchhoff Migration, or for pre-stack Kirchhoff Migration followed by CMP stacking. Figure 8 shows the CMP stack of the pre-processed model data using the VRMS velocity field from pass number six of autopicking (Figure 4), while Figure 9 shows the same data after the further step of post-stack Kirchhoff time migration.

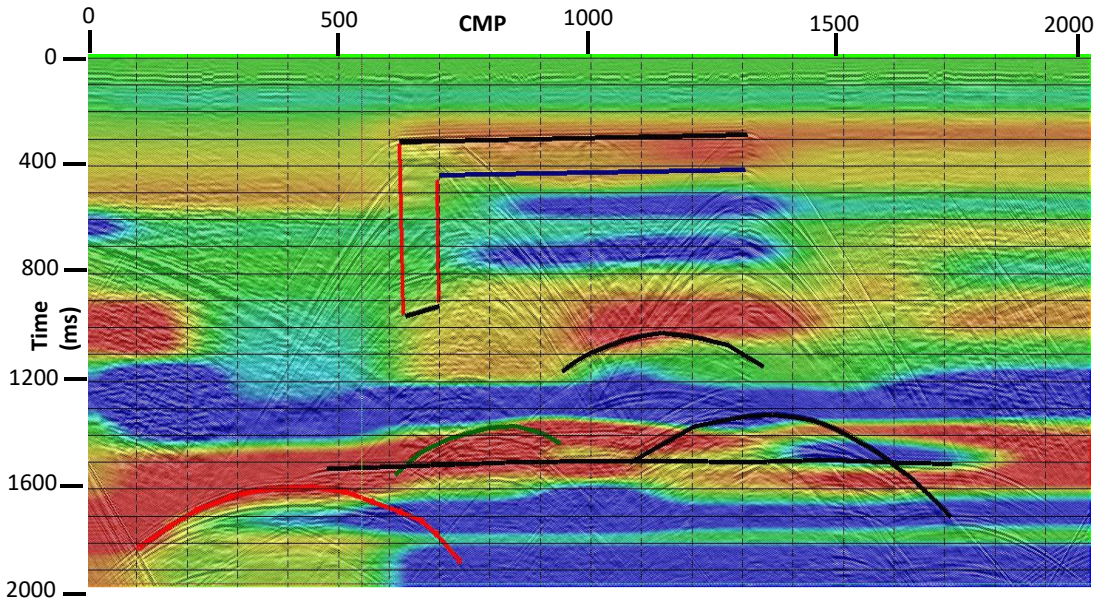

FIG. 7. Interval velocity vs. time (VIT) field created from the RMS velocity field in Figure 4. A few horizons are sketched in to show the relationship of the velocities to the structure. As can be seen, the correspondence is rough at best, and cannot be used for reliable migration. Interval velocity vs. depth (VID) cannot be created from the RMS velocity field by available algorithms, which yield negative or even imaginary velocities. Red = 6000m/s, blue = 500m/s.

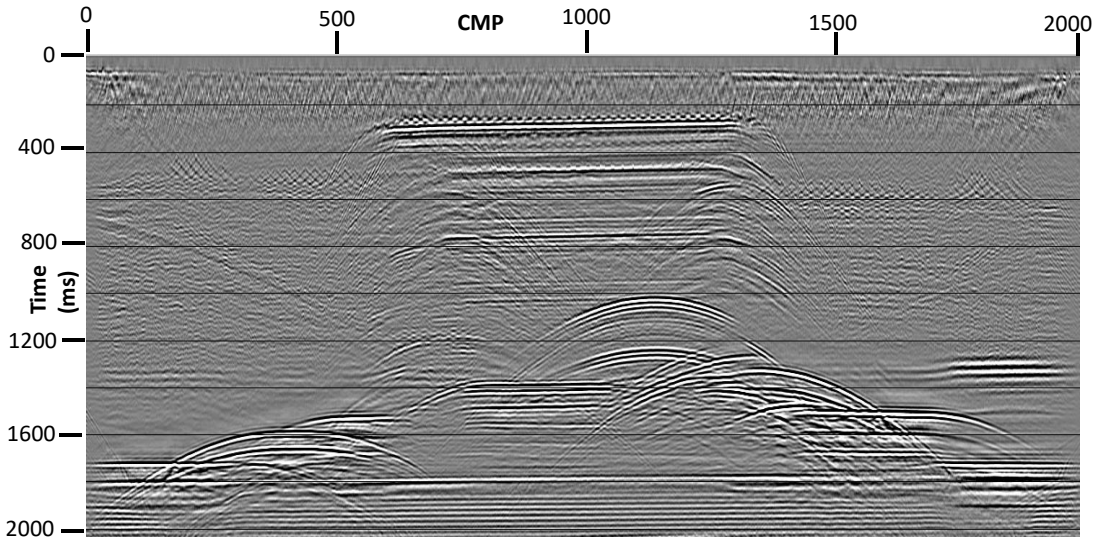

FIG. 8. CMP stack of the physical model data using the VRMS velocity field in Figure 4. Most reflection horizons can be seen in this image, indicating that NMO correction is successful.

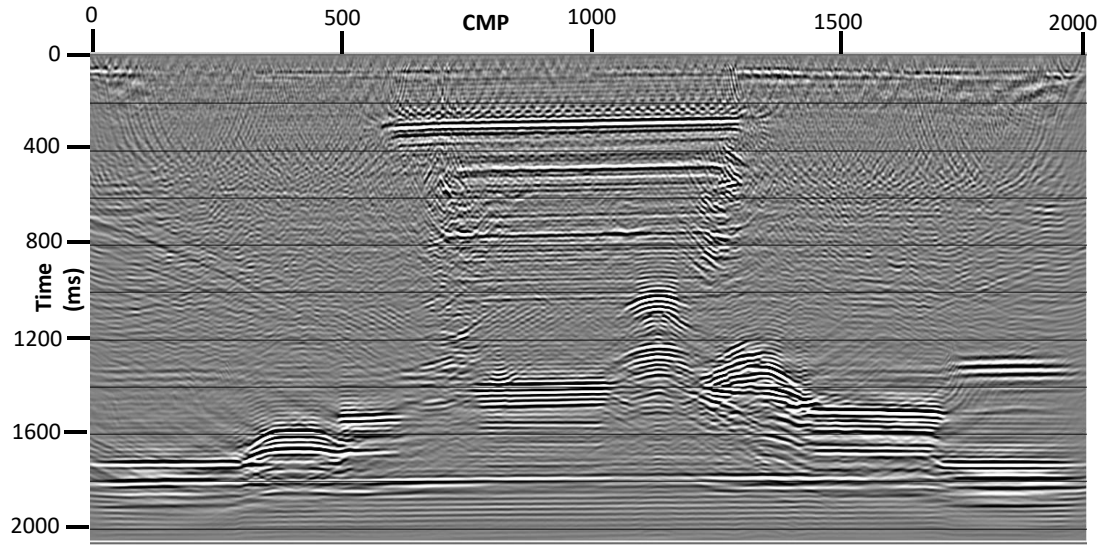

FIG. 9. Post-stack Kirchhoff time migrated CMP stack, using the VRMS velocities in Figure 4. Most of the interfaces in the model are visible, except for the vertical ones.

Since pre-stack Kirchhoff migration typically operates on common-offset gathers, several runs were made, using various ranges of offsets. We determined that offsets much beyond +/- 1000m contributed little to the final stack of the migrated results, and in fact, caused deterioration of the image. After some experimentation, we included only results for offsets less than +/- 600m. Figure 10 shows the result of Kirchhoff pre-stack time migration for offsets less than 600m. Using this image, as well as the one in Figure 9, we used the schematic in Figure 1 to pick all known interfaces in the physical model, as shown by the coloured horizons in Figure 11.

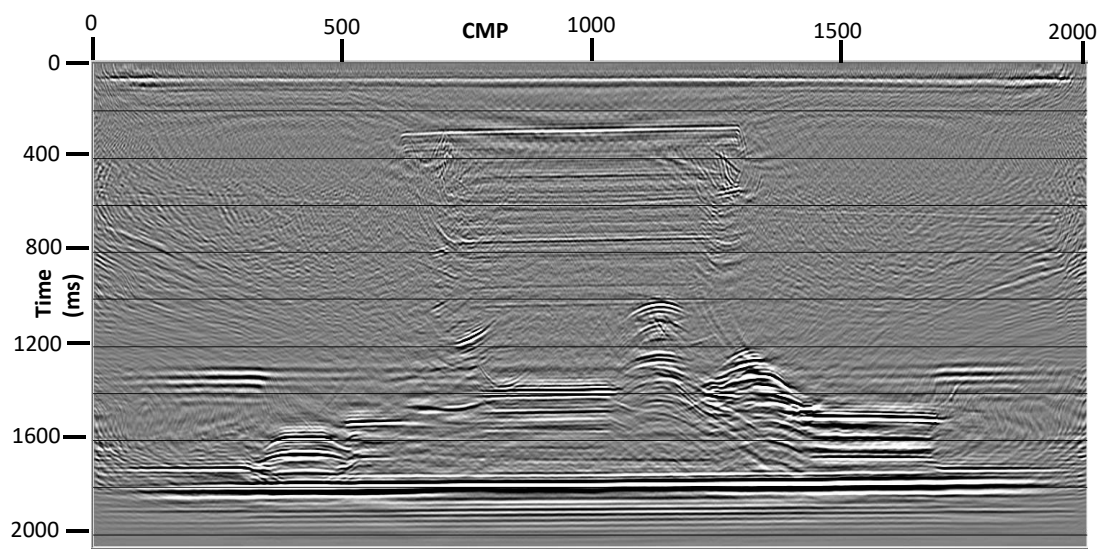

FIG. 10. Pre-stack Kirchhoff time migrated physical model data, using only absolute offsets less than 600m and the velocities from Figure 4. Features are very similar to the post-stack migration.

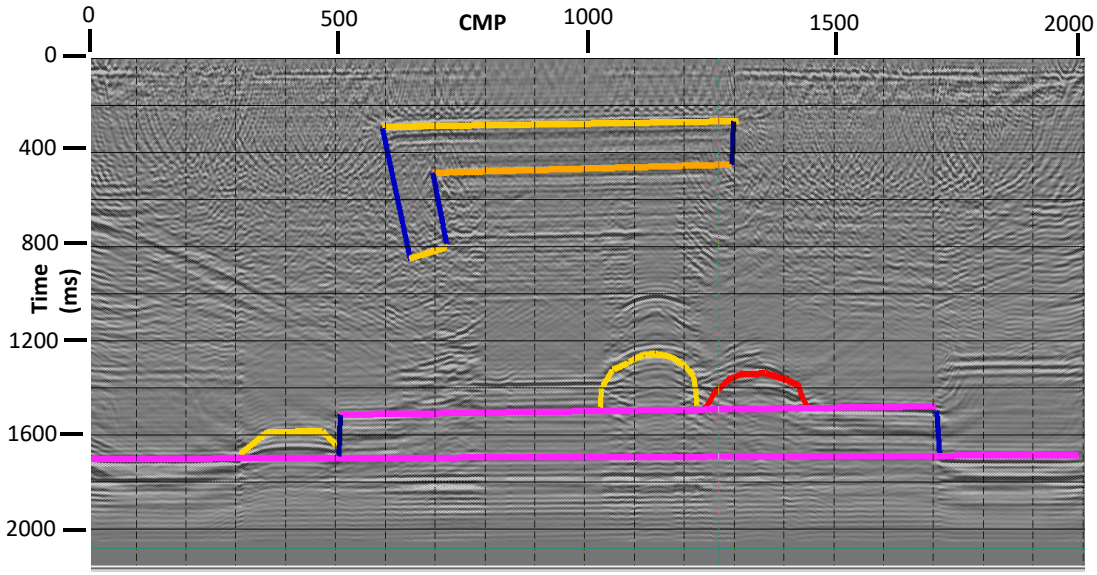

FIG. 11. Pre-stack Kirchhoff time migrated section with known model horizons picked and overlaid. The correspondence between image and schematic horizons is quite good.

Since the picked interfaces shown in Figure 11 are all expressed in travel time, we can post them to a blank interval velocity vs. time (VIT) field, and use the velocity editing function in the SeisSpace volume viewer application to fill the spaces between picked horizons with the known values of velocity from the actual physical model. This results in the interval velocity vs. time (VIT) field shown in Figure 12. This field can be converted to interval velocity vs. depth (VID), as shown in Figure 13, where we can see distortions in boundaries of the velocity model features, caused by the non-linear conversion from VIT to VID. After the boundaries have been manually adjusted, and the velocities re-filled into the defined spaces, the resulting interval velocity vs. depth model (VID) is as shown in Figure 14.

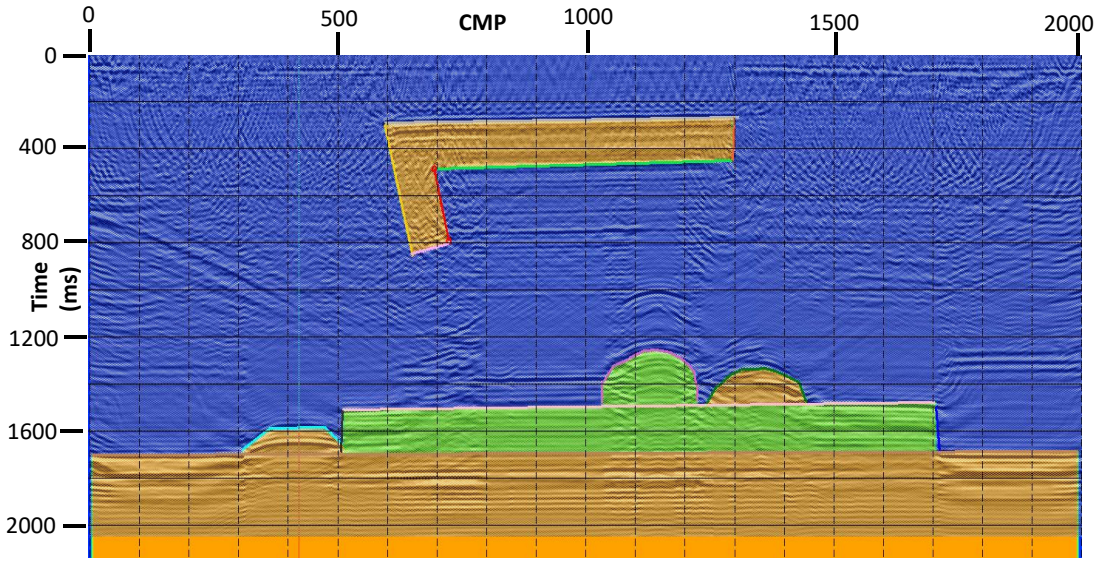

FIG. 12. Volumes between picked horizons filled with known constant velocities from physical model properties. This is the interval velocity vs. time (VIT) digital model representation. Image in the background is the pre-stack time migration based on the RMS velocity field in Figure 4.

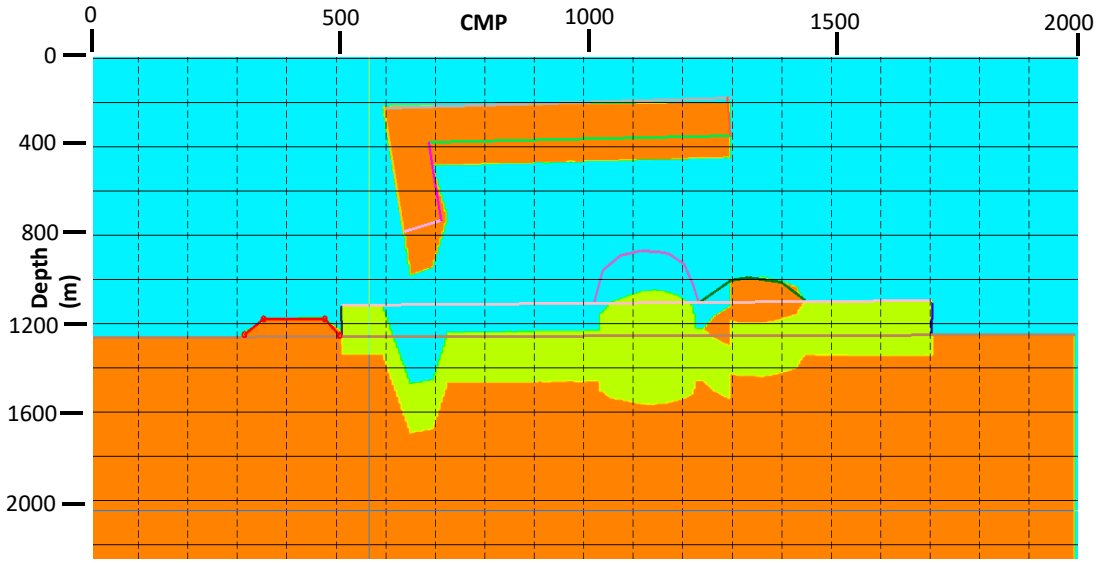

FIG.13. Interval velocity vs. depth (VID) velocity field, converted from the interval velocity vs. time (VIT) field in Figure 12. It is obvious that the model feature boundaries must be manually adjusted to conform to their actual configurations.

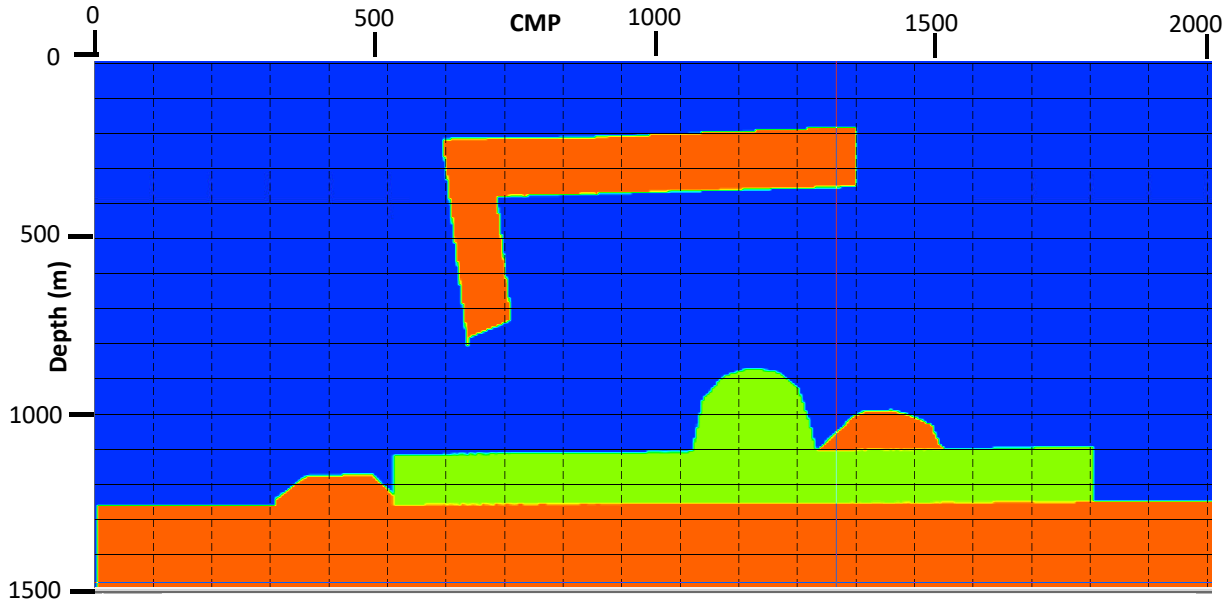

FIG. 14. The final interval velocity vs. depth model, after model feature boundaries have been adjusted, and correct velocities re-filled into the defined spaces.

The interval velocity vs. depth can be converted to VRMS for stacking, as shown in Figure 15, and a new CMP stack created, as in Figure 16, as well as a new version of post-stack Kirchhoff migration in Figure 17. These can be compared with Figures 8 and 9, respectively. The picked model horizons can be overlaid on Figure 17 and adjusted, if necessary. When we performed this exercise, we determined that no significant adjustments were warranted for the picked horizons. An important lesson to be taken from this is that the CMP stack image, as well as the post-stack migrated image, are relatively insensitive to the VRMS velocity field used to correct NMO and to migrate the data. If we compare Figures 8 and 16, as well as Figures 9 and 17, we see that the relatively minor differences in the images don't seem to reflect the major differences in the VRMS velocity fields used to create them (Figure 4 vs. Figure 15).

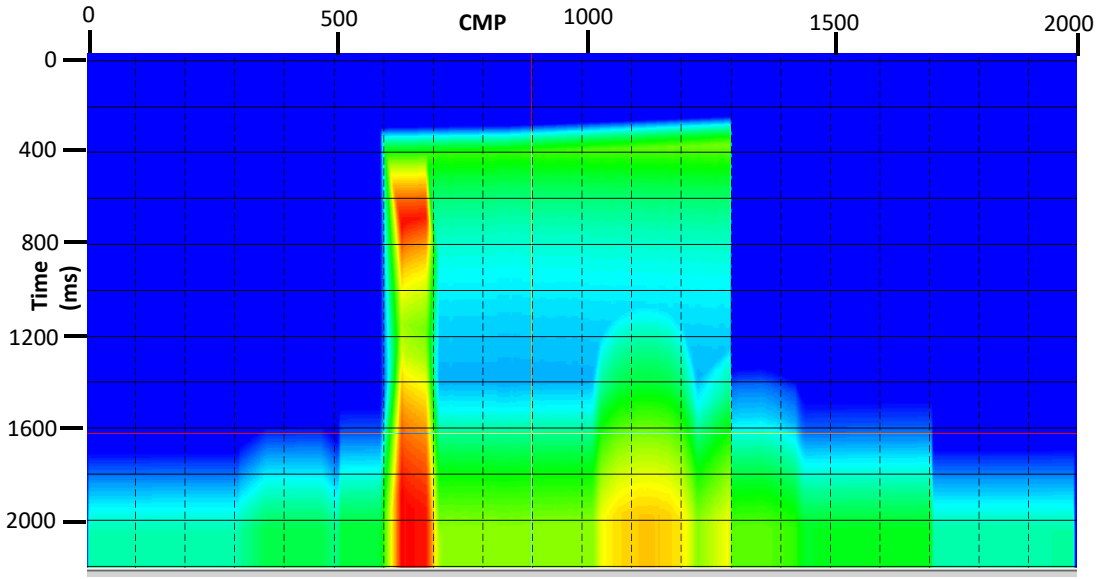

FIG. 15. VRMS stacking velocity field created from the model velocities in Figure 13. Compare with Figure 4.

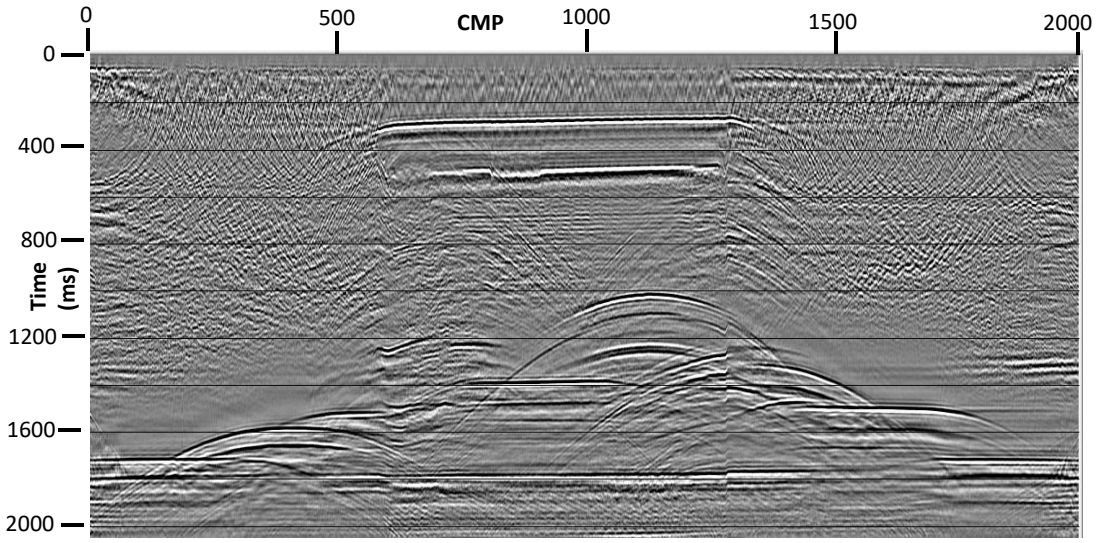

FIG.16. CMP stack of physical model data using the VRMS velocity field in Figure 15. Compare with Figure 8.

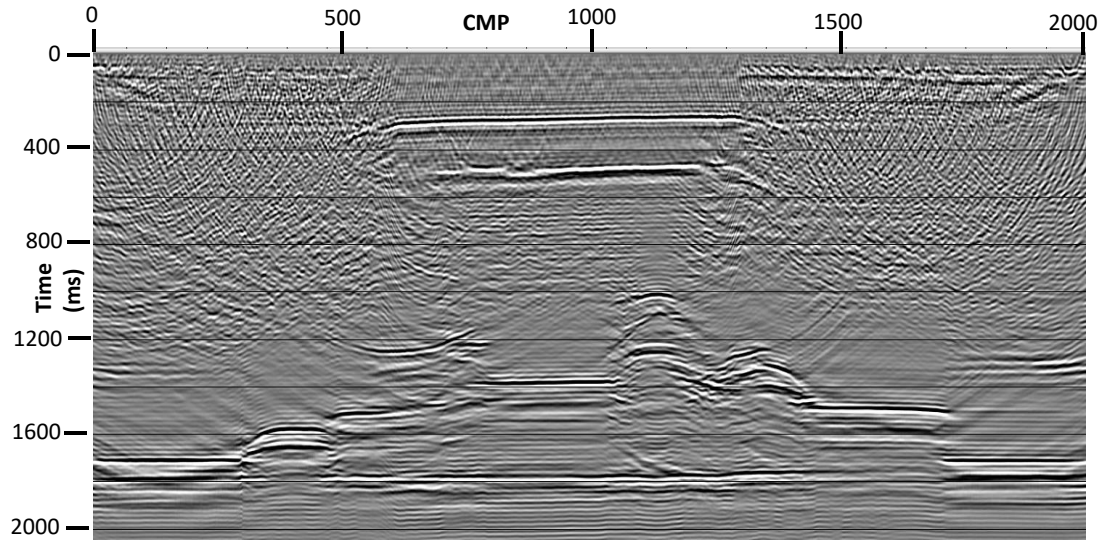

FIG. 17. Post-stack Kirchhoff time migration of CMP stack in Figure 16, using VRMS velocities in Figure 15. Compare with Figure 9.

Forward modeling of the digital velocity model

One way to determine how well our digital model conforms to reality is to use it in a numerical modeling procedure to estimate the seismic data that the model would generate during a survey using the same geometry as the actual laboratory survey on the scale model. A comparison of the forward-modeled seismic data with the processed physical model data should give us insight as to the veracity of our processing, as well as our modeling. The finite difference modeling algorithm we chose is a module in SeisSpace (Kelly et al 1976, Kelly et al 1990) which generates an acoustic response to a model represented as a digital velocity field, as well as an optional density field. The acoustic modeling is appropriate in this case, since the physical model itself incorporates water as the largest component by volume, and therefore doesn't support an elastic response. During our modeling efforts, we were unable to get the algorithm to accept a density field, so the responses we show are based on velocity alone. This means that the kinematics of the response should be largely correct, but the amplitudes do not reflect true acoustic impedance changes. In addition, our digital model does not incorporate out-of-plane interfaces corresponding to the sides or ends of the physical modeling tank, so the simulated seismic records will lack events corresponding to reflections from those missing features, as seen in the physical model records.

Comparing the two realities

Most Full Waveform inversion procedures compare the output of seismic processing on measured seismic response data with the output of forward modeling by computing a residual between the two results, often a sum of squared differences of seismic amplitudes. The usual process is to minimize the residual by computing successive adjustments to the model parameters which cause the model seismic response to more closely resemble the real seismic response. In the present study, we do not have a minimization algorithm, so our analysis is just a visual comparison of the seismic response recorded during the physical modeling experiment to that computed from our best digital representation of the

physical scale model. We compare single shot records as well as stacked and migrated images, and comment on the differences observed. As a test of the sensitivity of the numerical modeled response to the details of the digital input model, we show single gathers and stacked images for a velocity model similar to the 'real' model, but with some boundary disturbances.

COMPARISON RESULTS

Seismic response comparison

We first present individual shot gathers from the physical model and the comparable shot point in the finite difference model. Figure 18 shows the raw shot gather at source point 301 from the physical model experiment, with no processing. It is apparent that the direct water arrival and its reverberations are by far the strongest events on this gather, although we see evidence of other events in the background. We apply a radial trace filter to attenuate these arrivals and obtain Figure 19. In this figure we observe a strong hyperbolic event, whose apex is at about 550ms, which we can identify as a broadside reflection from the sides of the modeling tank. Likewise, we observe an end-on reflection from the near left end of the modeling tank entering the gather at about 900ms. If we had displayed data at deeper times, we would also see a reflection from the tank bottom. There are also lots of coherent dipping events contaminating the shot gather, likely related to water-borne reflections and reverberations. Nevertheless, we can also observe various coherent events, both shallow and deep, that are reflections from the features of the physical model. The comparable shot gather from source point 301 in the numerical model is shown in Figure 20. We have applied the same RT filter as for the data in Figure 19 to suppress the direct arrivals, as shone in Figure 21. The reflections from various model features are quite visible on this display, due to the lack of coherent background noise created in the modeling tank environment (there was no easy way to model the out-of-plane tank boundaries for the 2D finite difference algorithm). We were also not able to incorporate the density into the finite difference modeling, so reflection amplitudes are not correct, even though kinematics for the events should be. Comparing Figures 19 and 21 shows reasonable correspondence between model features. Figure 22 shows the physical model shot gather for the shot position 501 in the centre of the model. On this gather, the reflection events are much more prominent, in spite of the background noise. Figure 23, the comparable shot from the numerical model, shows a significant agreement with the details of reflections seen in Figure 22, except for the tank boundary reflections, and the reverberations evident in the physical model events.

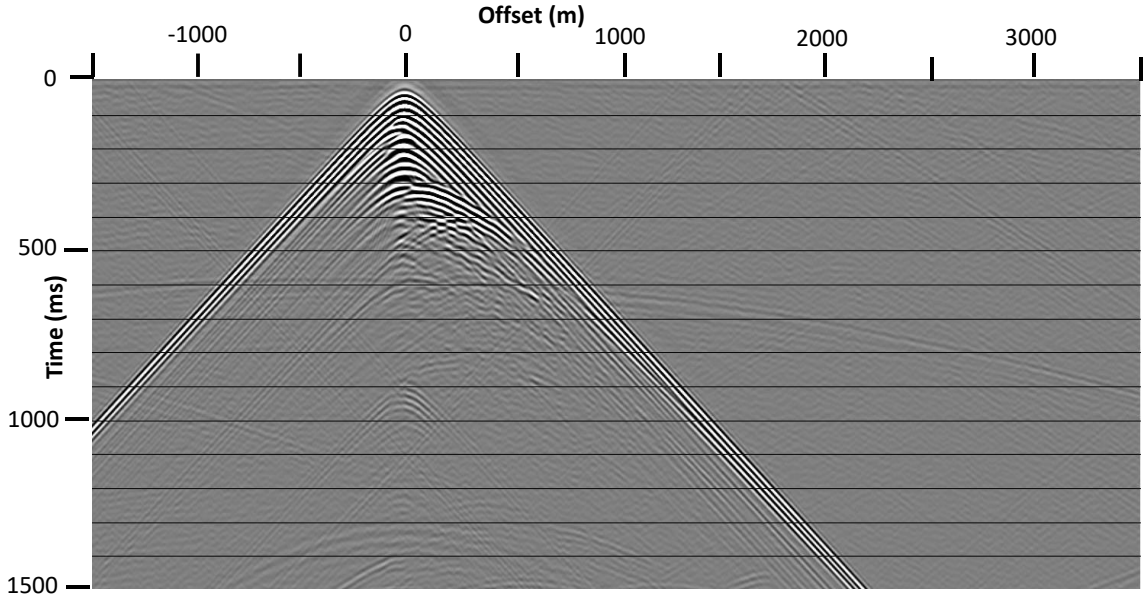

FIG. 18. Physical model shot gather for source point 301. Note that the direct water-borne arrival dominates this record.

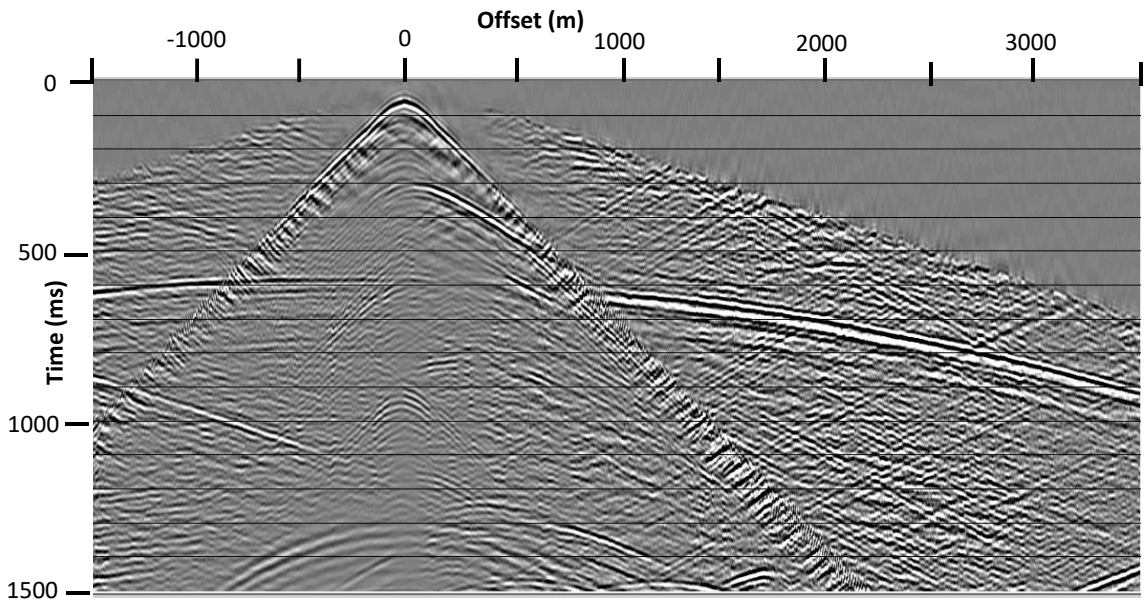

FIG.19. Physical model shot gather for source point 301 after RT filtering to attenuate the direct arrival, as well as Gabor deconvolution to whiten the wavelet. Broadside tank reflections have not been attenuated at this point.

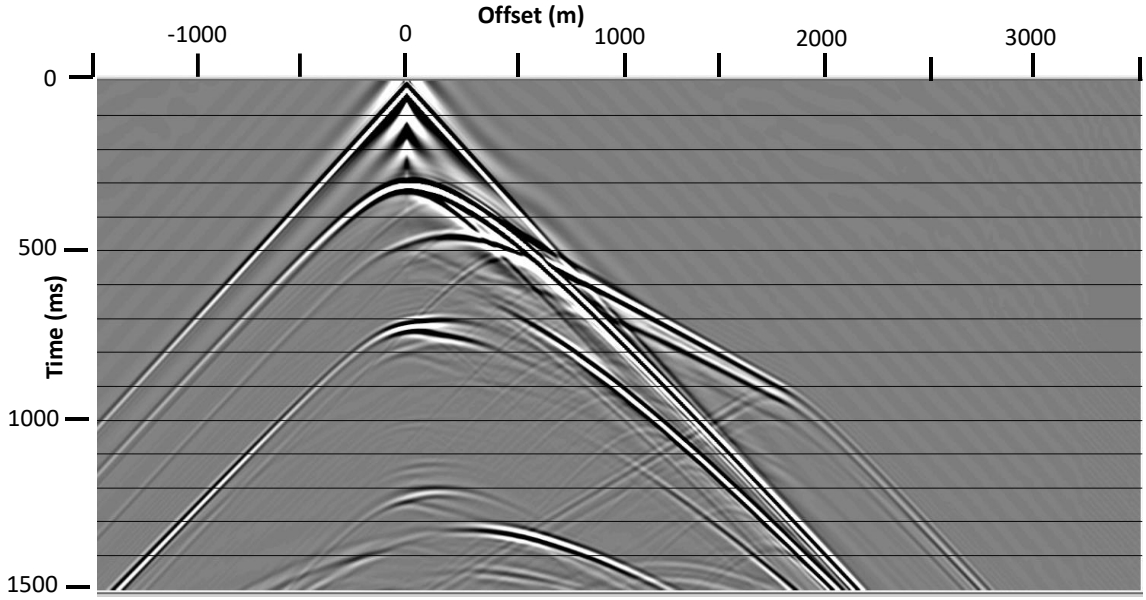

FIG. 20. FD numerical model shot gather for source point 301. Although the water-borne arrival is strong, the underlying reflections are easily visible.

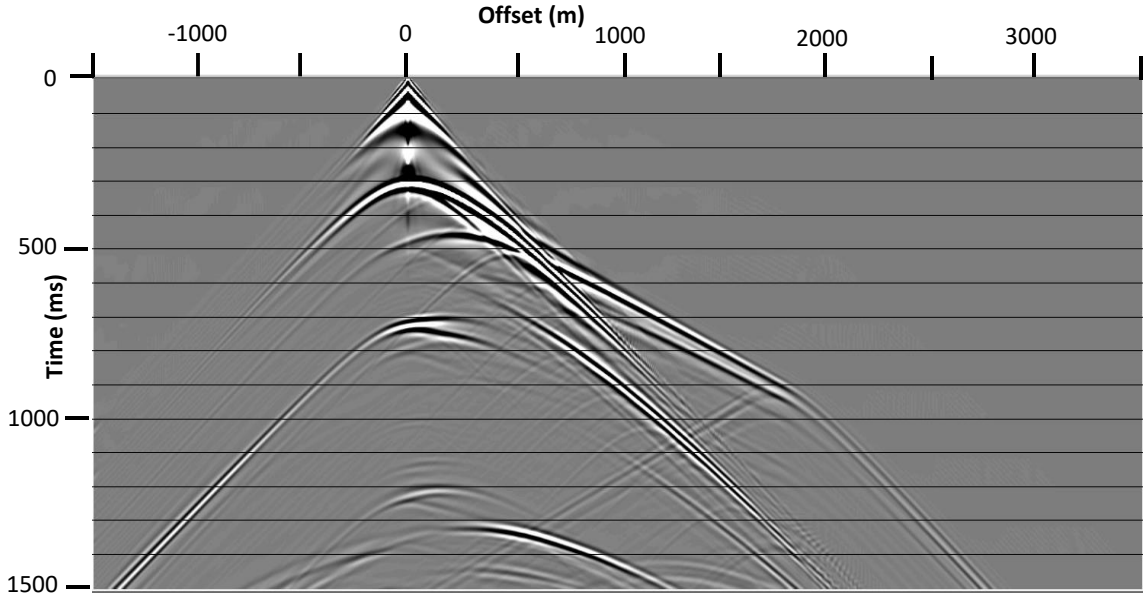

FIG. 21. FD numerical model shot gather for source point 301 after RT filtering to attenuate the water-borne energy.

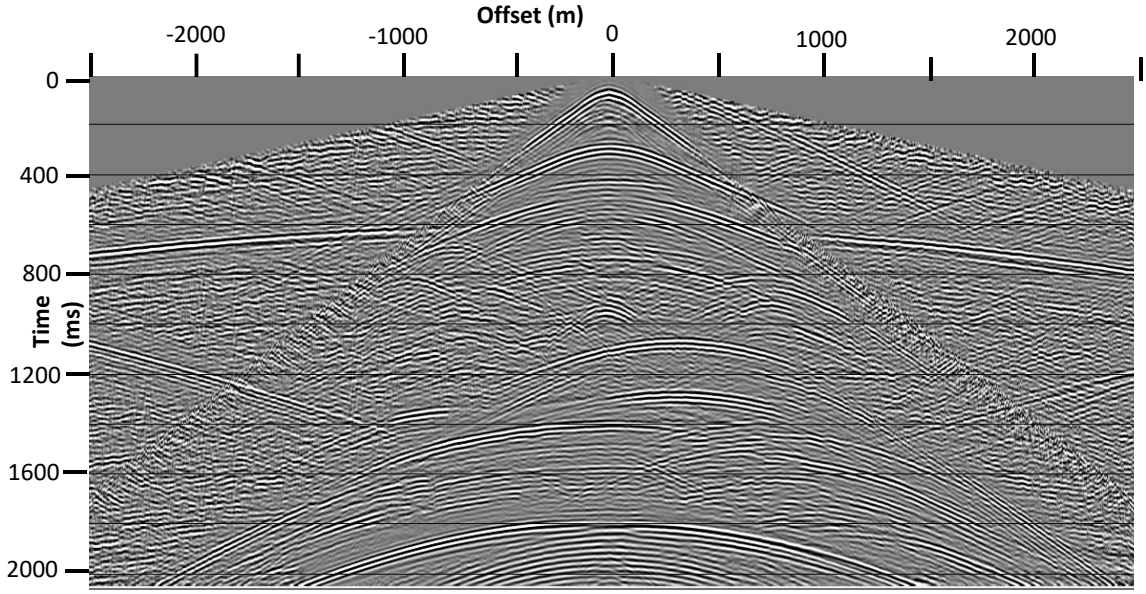

FIG.22. Physical model shot gather for the centre of the physical model at source point 501. RT filtering and Gabor deconvolution have been applied.

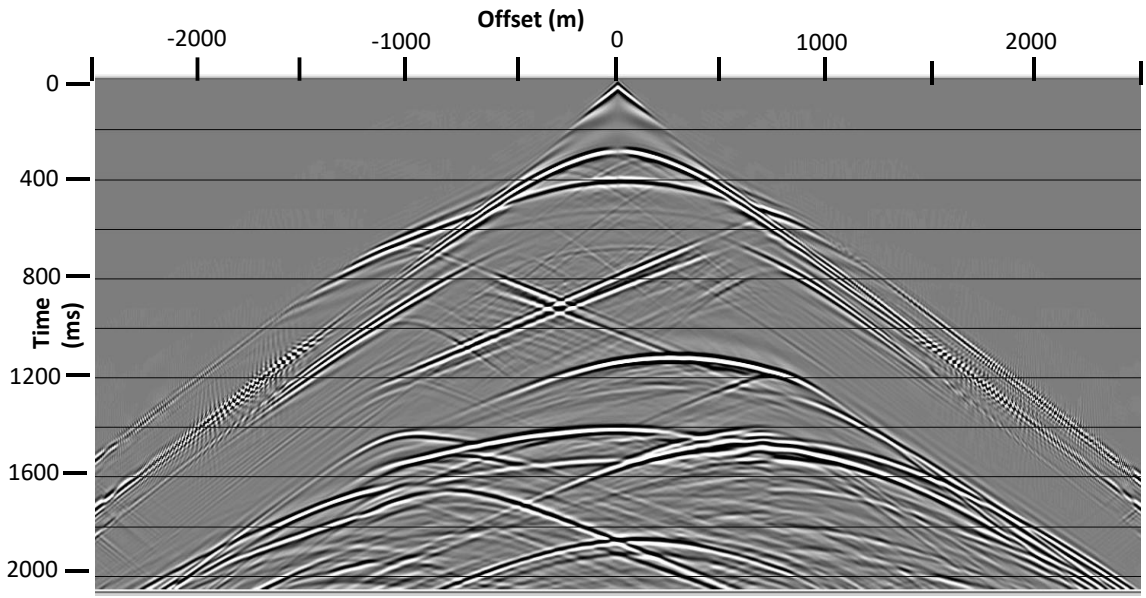

FIG. 23. FD numerical model shot gather for source point 501. RT filtering has been applied to attenuate direct arrivals. Most events correspond to events seen in Figure 21, except for amplitude.

Seismic CMP image comparison

The best images to compare for the two data sets are the pre-stack Kirchhoff depth migration results, which we obtain using the same digital model velocities. This type of migration is best applied in the common-offset domain, so we experimented with different values of maximum offset, while using the maximum allowable migration aperture. Interestingly, we found that absolute offsets greater than about 1000m contributed very little to the final stack image, for either data set; including results for absolute offsets in the

300m to 600m range produced the best images. Although we recorded data for both the physical model and the numerical model for a full range of offsets out to 5000m, only a small portion of the data contributed to meaningful images, even for a CMP stack, due to the low velocities and NMO stretch distortion. The post-stack Kirchhoff time migration, shown in Figure 11, that was used to pick and place the known physical model boundaries, used only absolute offsets less than 600m.

Figure 24 shows the pre-stack Kirchhoff depth migration results for the physical model data, using absolute offsets less than 600m, while Figure 25 shows the same results overlaid on the digital velocity model. Of interest in these images is the fact that the dike and sill structure appear to prevent complete illumination of the dome structure centred at CMP 1100, particularly its left flank; but the dike itself can be clearly seen because of what are likely wave modes trapped inside the dike itself. It is also clear from these images that the dike shadows the deep layers beneath it. Figures 26 and 27 show the corresponding images for the finite difference data. These images are quite similar to those from the physical model, except much cleaner, as we expect. Two important differences, however: the flanks of the three dome structures are much better imaged by the numerical model than the physical model, and the dike, while clearly visible, shows no internal modes, but does exhibit a reflection from its deep end. As a matter of interest, we compare the depth-migrated zero-offset gather (single fold) from the physical model in Figure 28, with the migrated zero-offset gather (also single fold) from the numerical data in Figure 29. In both cases, the dike structure is clearly visible, even though it is unlikely that any reflection energy from its sides contributes to the image in either case.

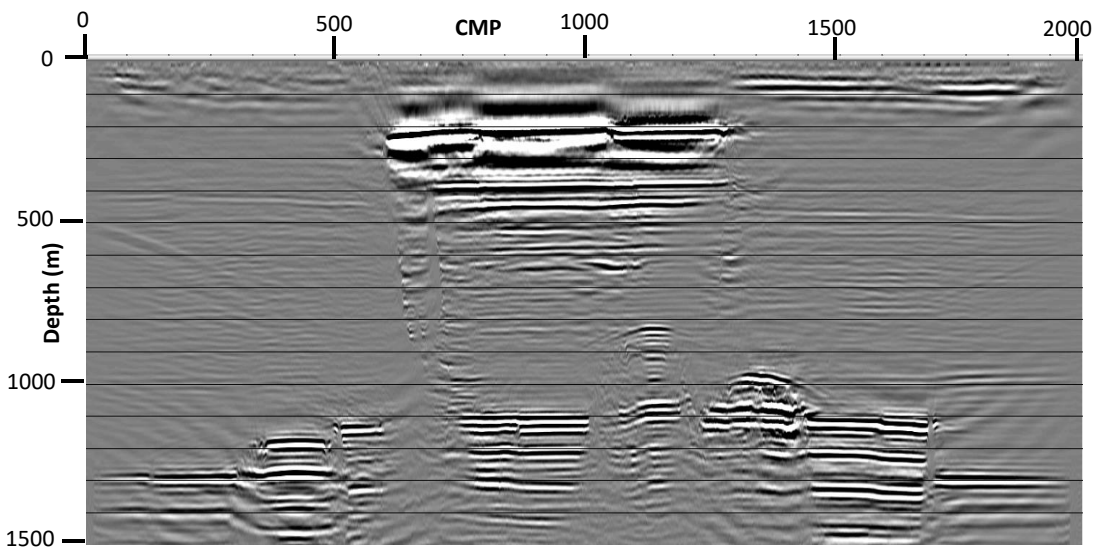

FIG. 24. Pre-stack Kirchhoff depth migration of physical model data using the exact model velocities in Figure 14. Low frequencies have not been attenuated.

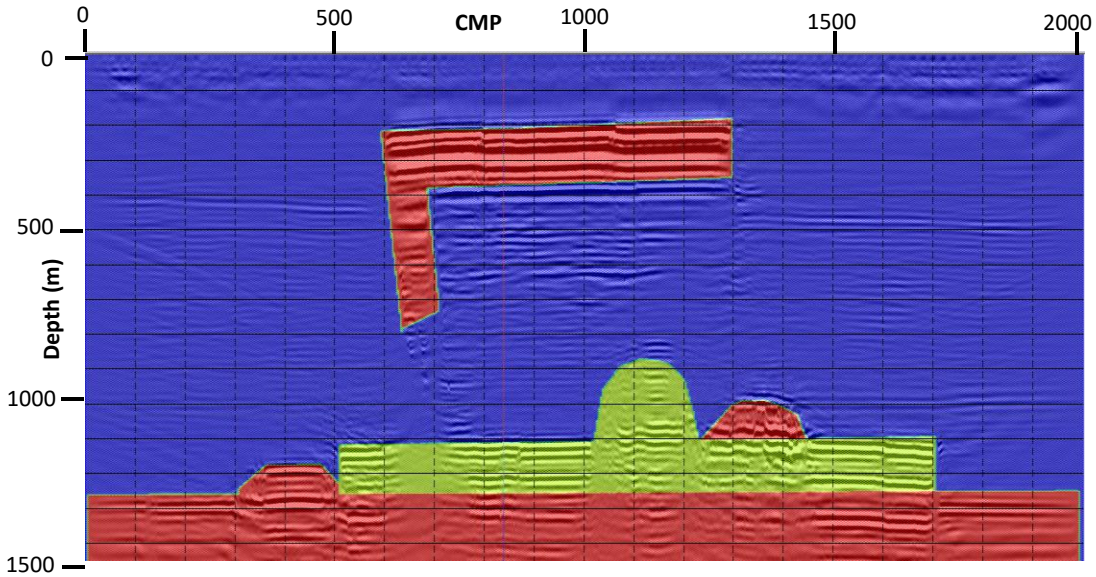

FIG. 25. Pre-stack Kirchhoff depth migrated physical model image overlaid on the exact velocity model used for the migration. Blue = 1485m/s; yellow = 2350m/s; red = 2745m/s

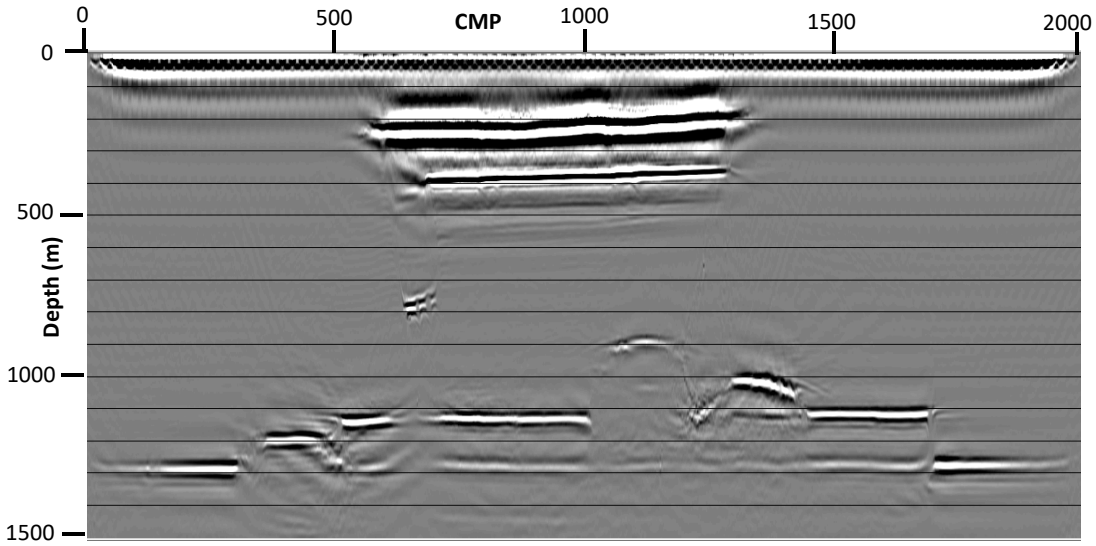

FIG. 26. Pre-stack Kirchhoff depth migrated FD numerical model, migrated with the exact model velocities in Figure 14. Image is much cleaner than that in Figure 24, since there are no tank reflections or reverberations in the numerical model.

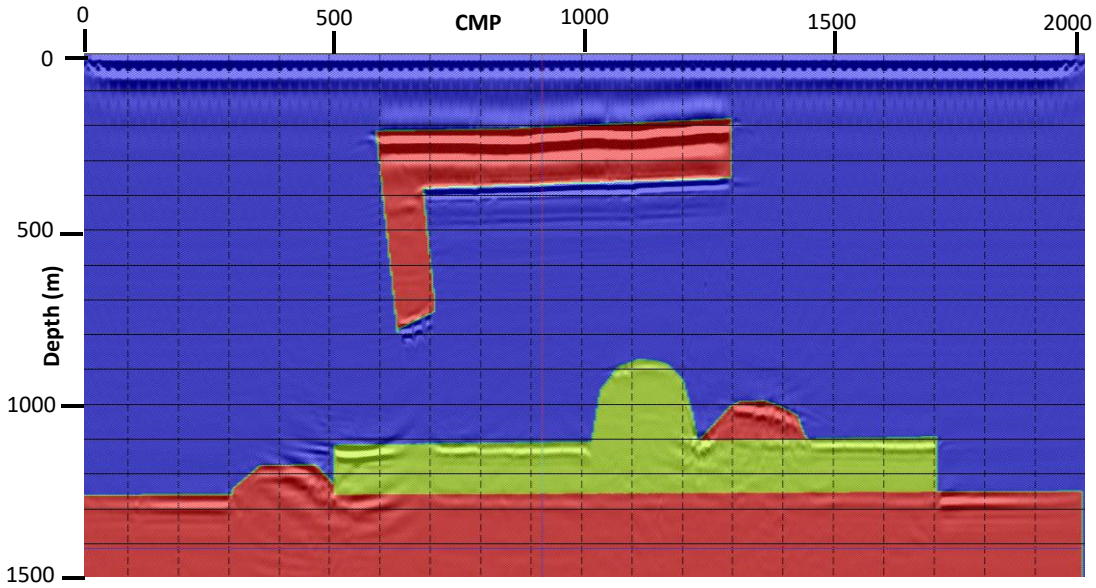

FIG. 27. Pre-stack Kirchhoff depth migrated FD numerical model image overlaid on the exact model velocities used to migrate the data. Blue = 1485m/s; yellow = 2350m/s; red = 2745m/s

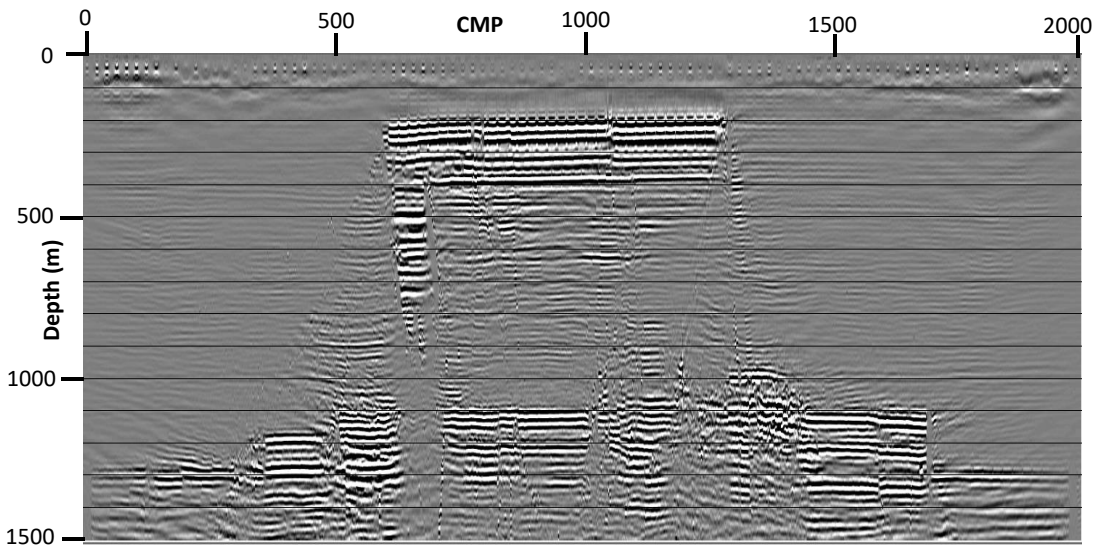

FIG. 28. Pre-stack Kirchhoff depth migrated zero-offset gather for the physical model data. Note the surprising visibility of the vertical dike, and the shadow it casts on the deeper layers. Obviously, there are no reflections from the vertical sides of the dike, but trapped modes inside the dike make it visible. All vertical boundaries in the model are surprisingly visible.

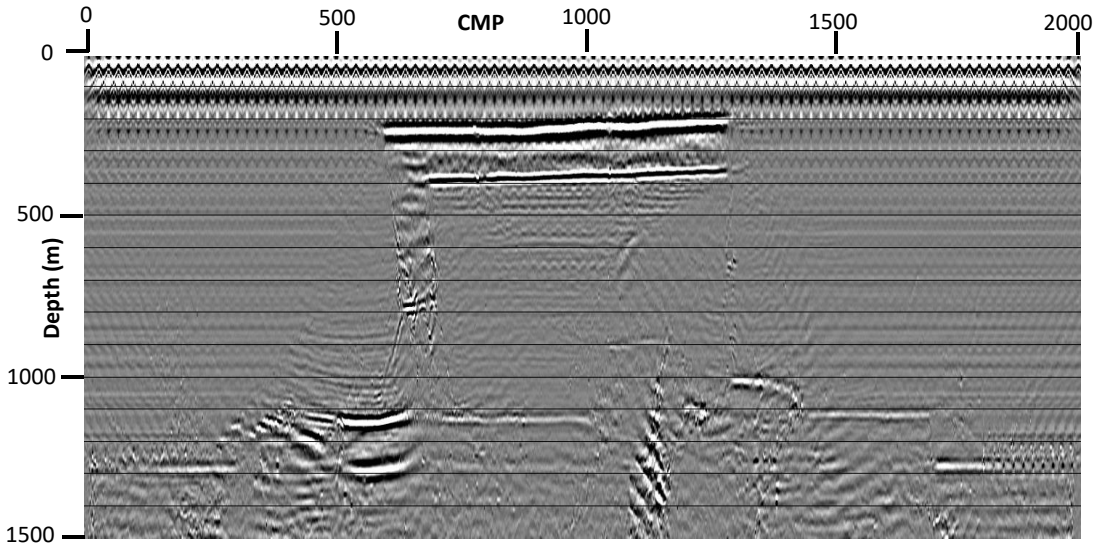

FIG. 29. Pre-stack Kirchhoff depth migration of zero-offset panel FD numerical model. In this image, as well, all the vertical boundaries are visible as event terminations or texture changes. The dike is easily visible and even manifests a reflection from its deep end.

Sensitivity to velocity model in time

One interesting result in this study is that post-stack Kirchhoff time migration results differ very little from pre-stack time-migration results, as can be seen by comparing Figures 30 and 31. In addition, the time migration appears to provide better imaging of the flanks of the three dome structures. Of interest, as well, is the fact that Kirchhoff time migration results are relatively insensitive to the VRMS velocities used to produce them. Figure 32 shows the post-stack Kirchhoff time migration using the best estimated autopicked VRMS velocities, while Figure 33 shows the same results using the exact VRMS velocities obtained from the exact digital model (Figures 4 and 14). The most noticeable difference in these images is that the model interfaces are cleaner and slightly better resolved on the image using the exact RMS velocities.

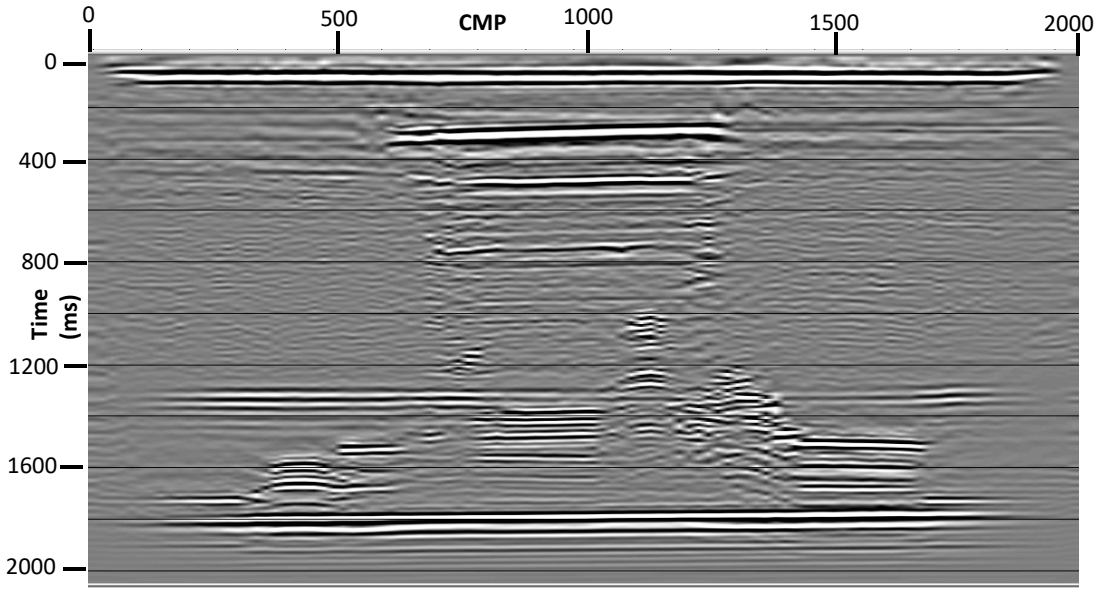

FIG. 30. Post-stack Kirchhoff time migration of physical model—anti-alias applied.

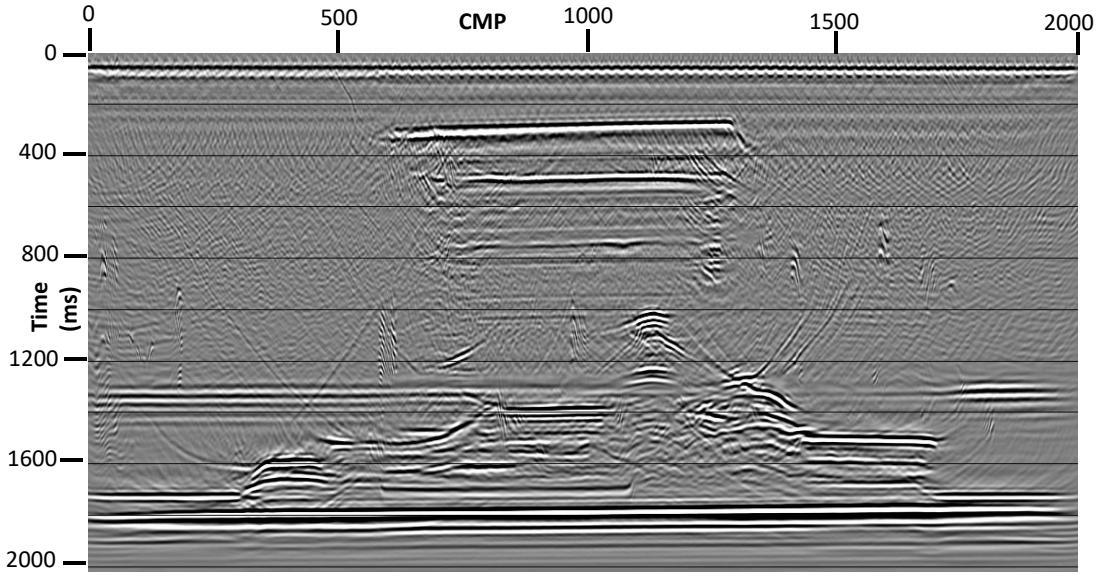

FIG. 31. Pre-stack Kirchhoff time migration of physical model—no anti-alias applied.

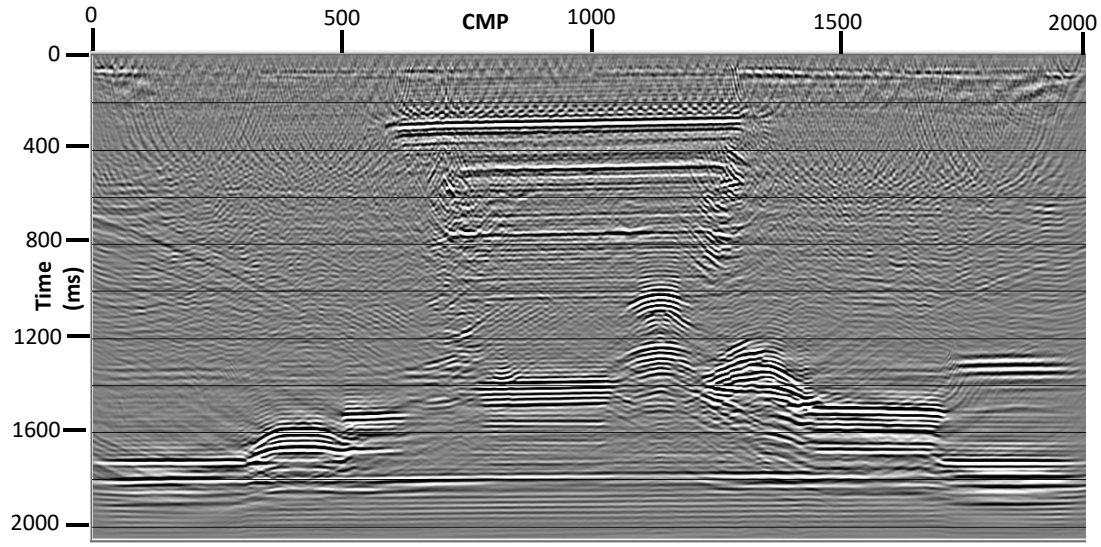

FIG. 32. Post-stack Kirchhoff time migration of physical model data using the best autopicked VRMS velocities from Figure 4.

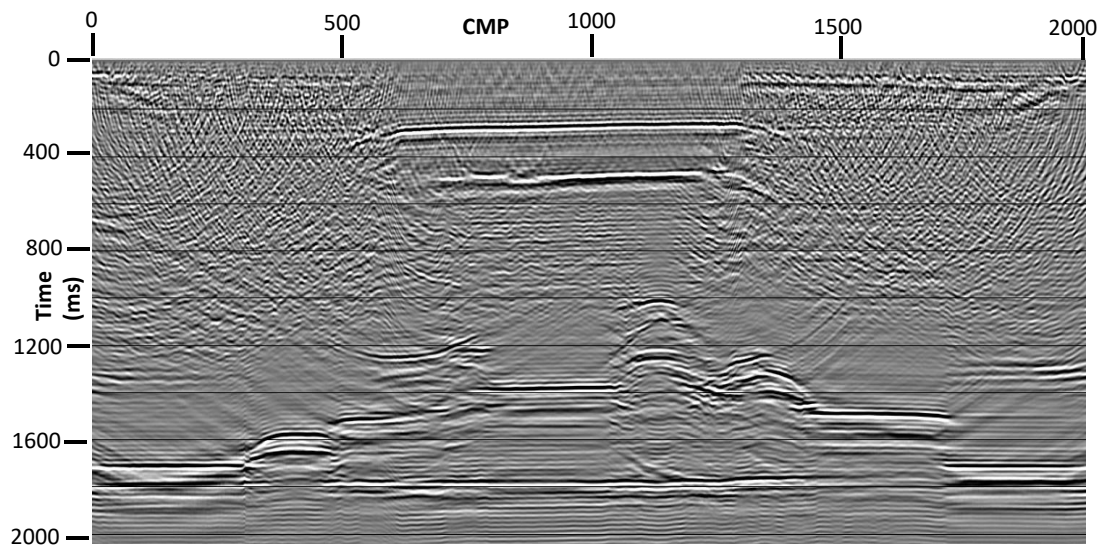

FIG. 33. Post-stack Kirchhoff time migration of physical model data using the VRMS velocities from the exact model (Figure 15).

Sensitivity of numerical modeling to digital model boundary errors

In a previous section, we compared physical model responses and images with numerical model responses and images, where the underlying digital model for the numerical results is exactly the one confirmed by the physical model images. In this section, we compare numerical model results and images for the exact digital model and a model which contains errors in the geometry of the boundaries, shown in Figure 34.

We show in Figure 35, the shot gather corresponding to the same shot location as that in Figure 23. The comparison reveals very significant differences in the seismic responses,

indicative of the perturbed layer boundaries in Figure 34. If we process the entire modeled profile using this erroneous velocity model, we obtain the pre-stack Kirchhoff depth migrated section shown in Figure 36, which clearly does not correspond correctly to the actual velocity model shown in Figure 15, and overlaid in Figure 36. Compare with Figure 27, where the correct model boundaries are represented.

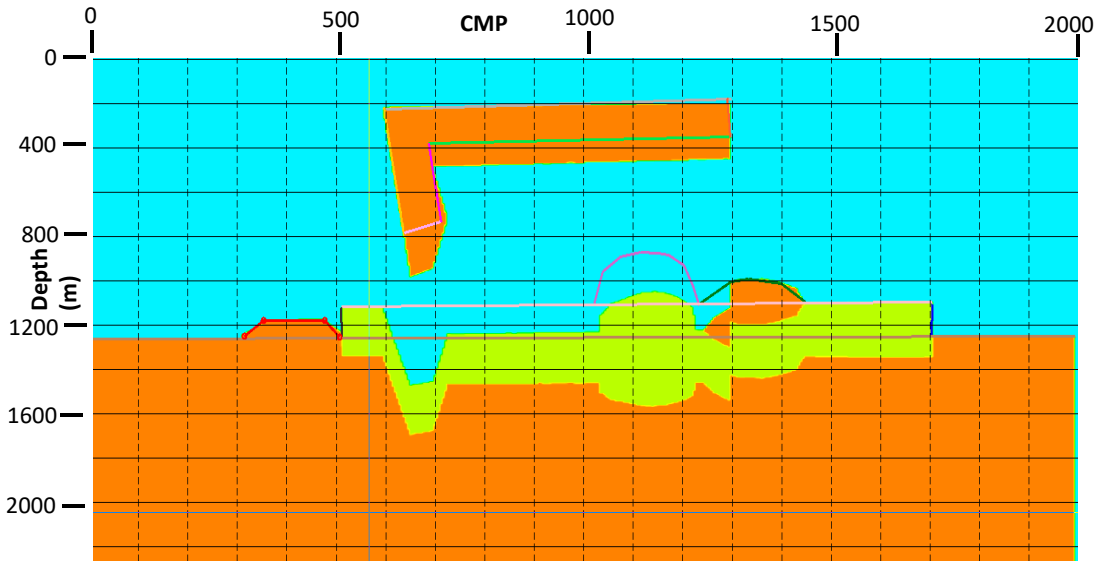

FIG. 34. Interval velocity vs. depth model with errors in the boundaries.

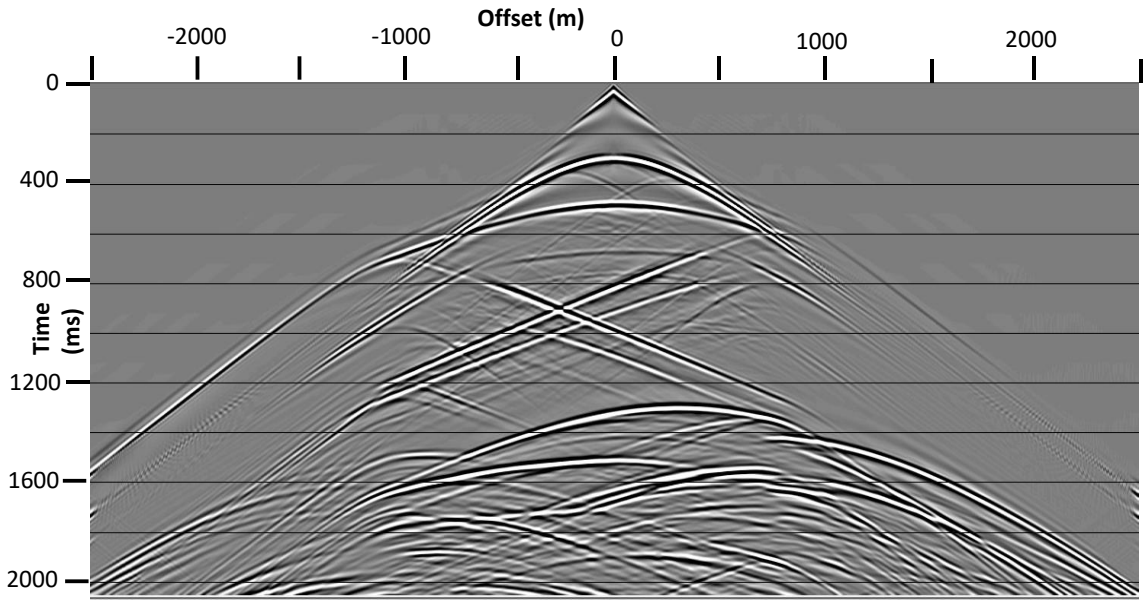

FIG. 35. FD numerical model shot gather from source location 501. Comparison with Figure 23 shows significant difference in reflection locations and shapes.

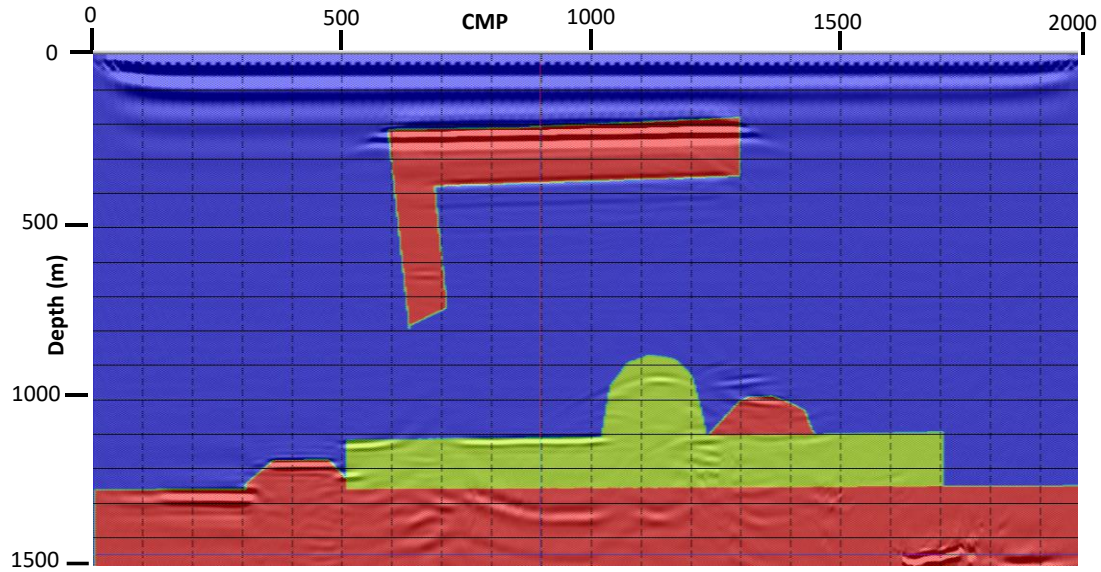

FIG. 36. Pre-stack Kirchhoff depth migration of FD numerical model of data from disturbed velocity model in Figure 34, correct velocity model overlaid. Compare with Figure 27. Discrepancies are obvious.

SUMMARY AND OBSERVATIONS

The purpose of this work has been to examine in detail the similarities and differences between seismic surveys created by a physical modeling survey of a scale model object and a finite difference modeling survey of a digital representation of the same scale model. Since we initially lacked the digital model representation, we first processed the physical model survey iteratively to obtain the best possible image. Our a priori knowledge about the model geometry and material properties was then imposed by picking the various model interfaces on the image and filling the intervening spaces with known material properties. After converting the resulting interval velocity vs. time model to interval velocity vs. depth, this digital model was used to produce final images for the physical modeling data, and it was also used with a finite difference numerical modeling scheme to produce a synthetic survey for direct comparison with the physical model images.

During this work, we made the following observations:

- Conventional NMO velocity analysis has difficulty with a model like this, which has relatively few reflecting interfaces, and major velocity inversions. Picking semblance maxima is difficult even with the guidance of a schematic model.

- VRMS stacking velocities apparently don't need to be very detailed in order to successfully stack and time-migrate these model data.

- VRMS velocities which successfully stack and migrate the model data aren't particularly useful in finding a realistic interval velocity model, either in depth or in time, due to the non-uniqueness of the inversion from VRMS to interval velocities.

- Time-migrated model images can be used successfully to orient the known physical model boundaries by picking, even when the images are created using relatively un-detailed VRMS velocities.

- Stacked and migrated images created using VRMS velocities from conventional NMO analysis don't differ much from the same images created using VRMS velocities from the exact digital model, except that the image interfaces using the exact VRMS are slightly better resolved. In other words, the time-migrated images don't have much discriminating power with respect to the correctness of the underlying digital VRMS model.

- There is not a lot of meaningful difference between images created by post-stack time migration and pre-stack time migration, as long as the same VRMS velocities are used for each.

- For this particular model, long-offset data were of little use in creating images, either CMP stacks or pre-stack migrations—there was very little useful image information on traces recorded at more than 1000m absolute offset.

- The physical model data contained events and noise not seen in the numerical model, due to reflections and reverberations from modeling tank walls and bottom. To some extent, these can be processed out. These might cause problems in a Full Waveform Inversion scheme, since this forward modeling scheme never creates them.

- We were unable to incorporate density into the numerical modeling, so reflection amplitudes were not accurately modeled. Nevertheless, numerically modeled reflection kinematics corresponded quite well to reflections observed in the physical model data.

- Migrated depth images of the physical model data and the numerical model data were similar in many respects, particularly in the conformity of the model boundaries to the modeling reflections.

- Features in the model with vertical orientation, like the high-velocity dike, are surprisingly visible in the pre-stack depth migrated images for both physical and numerical data, and especially visible on the migrated zero-offset gather. This is likely due to the visible termination of internal modes in the vertical feature at the feature boundary.

- The 'shadowing' effects of the dike and sill feature of the model were visible in both the physical model images, and to a lesser extent in the numerical model images.

- Distorted boundaries in the digital model were quite easily seen, not only on individual shot records, but on migrated images.

ACKNOWLEDGEMENTS

The author gratefully acknowledges the financial support of both CREWES and NSERC. Thanks, as well, to Halliburton for the use of donated SeisSpace software.

REFERENCES

Henley, D.C., 2003, Coherent noise attenuation in the radial trace domain, Geophysics, **68,** No. 4., pp 1408-1416.

Henley, D. C., and Wong, J., 2019, Let there be light: illuminating physical models from the surface: CREWES Research Report, 31, 22.1–22.27.

Kelly, K.R., Ward, R. W., Treitel, S., and Alford, R. M., 1976, Synthetic seismo-grams: a finite-difference approach: Geophysics, **41**, 2-27.

Kelly, K.R. and Marfurt, K. J., 1990, Numerical modeling of seismic wave propagation, Geophysics reprint series no. 13: Society of Geophysics.

Margrave, Gary F., Lamoureux, Michael P., and Henley, David C., 2011, Gabor deconvolution: estimating reflectivity by nonstationary deconvolution of seismic data, Geophysics, **76**, No. 3

Wong, J., Zhang, H., Kazemi, N., Bertram, K. L., Innanen, K. A. H., and Shor, R., 2019, Physical modeling of seismic illumination and SWD: CREWES Research Report, 31, 53.1–53.14.